QJEGH

Technical note

Quarterly Journal of Engineering Geology and Hydrogeology

Published Online First

https://doi.org/10.1144/qjegh2020-098

The thermal properties of the Mercia Mudstone Group

Dan Parkes[1], Jon Busby[1]*, Simon J. Kemp[1], Estelle Petitclerc[2] and Ian Mounteney[1]

[1] British Geological Survey, Keyworth NG12 5GG, UK
[2] Royal Belgian Institute of Natural Sciences, Geological Survey of Belgium, Rue Jenner, 13, 1000-Brussels, Belgium
JB, 0000-0002-4686-2963; SJK, 0000-0002-4604-0927; EP, 0000-0002-0131-8948; IM, 0000-0002-0295-9552
* Correspondence: jpbu@bgs.ac.uk

Abstract: The Mercia Mudstone Group (MMG) crops out extensively across England and Wales and its thermal properties are required for the design of infrastructure such as ground source heating and cooling schemes and electrical cable conduits. Data from the literature and new data from a borehole core have been compiled to generate an updated range of thermal conductivities related to rock type and the lithostratigraphy. These indicate a total range in saturated vertical thermal conductivity of 1.67–3.24 W m^{-1} K^{-1}, comprising 1.67–2.81 W m^{-1} K^{-1} for mudstones, 2.12–2.41 W m^{-1} K^{-1} for siltstones and 2.3–3.24 W m^{-1} K^{-1} for sandstones. These data are all from measurements on samples and there will be uncertainty when considering the thermal properties of the rock mass owing to micro- and macrostructural features. Geometric mean modelling of thermal conductivity based on mineralogy has overestimated the thermal conductivity. Correction factors for the modelled thermal conductivities have been calculated to allow a first estimate of MMG thermal conductivities when only mineralogical data are available. Measured thermal diffusivities from the borehole core were in the range of 0.63–3.07 × 10^{-6} m^2 s^{-1} and are the first measured thermal diffusivities to be reported for the MMG.

Received 20 May 2020; **revised** 9 September 2020; **accepted** 9 September 2020

The Mercia Mudstone Group (MMG) crops out extensively across England and Wales (see Fig. 1). From the south, it extends from east Devon, Somerset, the Bristol area and south Wales to the Gloucester and Worcester regions. Northwards, the outcrop broadens to underlie much of Warwickshire, Staffordshire and Leicestershire. To the east of the Pennines, it extends northwards through Nottinghamshire and Yorkshire and reaches the North Sea coast near Hartlepool. To the west of the Pennines, it underlies northern Shropshire, Cheshire and Merseyside, and the Formby and Fylde peninsulas, and farthest north crops out near Carlisle. Many towns and cities are underlain by the MMG including Cardiff, Bristol, Worcester, SE Birmingham, Leicester, Derby, Nottingham, Newark-on-Trent, Southport and Blackpool, where a knowledge of the thermal properties of the MMG is required for the design of infrastructure such as ground source heating and cooling schemes, underground thermal energy storage (UTES), tunnels and electrical cable conduits.

The purpose of this technical note is to provide an up-to-date account of the thermal properties of the MMG onshore UK. After an introduction to the lithostratigraphy of the MMG, existing thermal property data are reviewed followed by a detailed analysis of core from a recently completed borehole in the East Midlands. These new data provide calibration for estimates of thermal conductivity from mineralogical analyses, and finally all the data are combined to provide a 'best estimate' of MMG thermal properties.

It should be noted that the term mudstone implies a very fine-grained sedimentary rock in which the main constituents have grain sizes less than 63 μm, although the British Geological Survey suggests a grain size of less than 32 μm (Merriman *et al*. 2003). The primary components are clay minerals and quartz. However, the MMG has varied lithologies including some arenaceous units of silt- and sand-sized grains and overall it is probably more representative of a silty mudstone.

The Mercia Mudstone Group

A revision of the lithostratigraphic nomenclature for the MMG was published by Howard *et al*. (2008) and replaced that of Warrington *et al*. (1980). This new nomenclature is referred to as the revised lithostratigraphy and a simplified description is given here. This simplified description provides the geological framework for the thermal properties and is intended to be used without expert geological knowledge. The onshore MMG of England and Wales comprises red, and less commonly green and grey mudstone and siltstone. Halite deposits occur in Dorset, Somerset, Worcestershire, Staffordshire, Cheshire, west Lancashire and south Cumbria, and east and north Yorkshire. Sulphate deposits of gypsum and anhydrite, and sandstone beds are common at some stratigraphic levels, but are a minor constituent of the Group. Table 1 presents the formation nomenclature for the MMG with a brief lithological description taken from the British Geological Survey's (BGS) Lexicon of Named Rock Units (https://www.bgs.ac.uk/lexicon/?src=topNav). In many regions, formations are subdivided into members, many of which correspond to formations in the replaced lithostratigraphy of Warrington *et al*. (1980), although these are not referred to here. Howard *et al*. (2008) gave the full lithostratigraphy for the 10 regions shown in Figure 1. Rock types referred to in Table 1 and subsequent tables are explained in Table 2.

Laboratory testing for thermal conductivity (and diffusivity) of a sample depends on mineralogy, porosity, pore filling fluid and microstructure. This may differ from the thermal conductivity of the rock mass where macrostructures (e.g. bedding, fractures, etc.) also have an influence. A thermal response test (TRT) conducted in closed-loop boreholes drilled for the installation of ground source heat pumps measures an apparent thermal conductivity for the rock mass. A TRT can be affected by advective heat transfer owing to groundwater flow and hence this apparent thermal conductivity may differ from the intrinsic thermal conductivity of a sample or the rock mass. Thermal conductivity is a tensor and the value measured horizontally will often differ from that vertically owing to anisotropy within the rock. This often occurs in layered sedimentary rocks especially those composed of platy minerals such as clays. Bloomer (1981) in measurements of thermal conductivity of United Kingdom mudrocks found the thermal conductivity measured parallel to bedding was 1.19–2.17 times higher than that measured

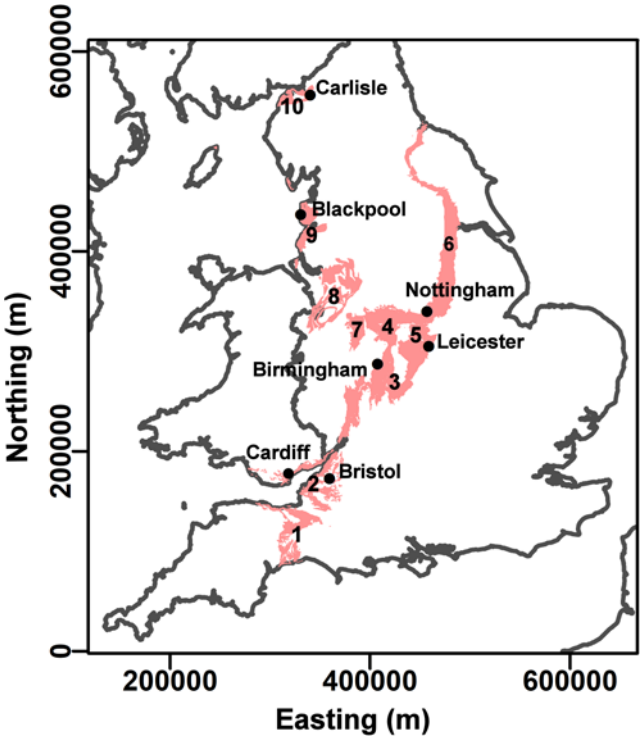

Fig. 1. Outcrop of the Mercia Mudstone Group in England and Wales. The numbered regions are as follows: 1, Wessex Basin; 2, Bristol–South Wales; 3, Worcester–Knowle Basins; 4, Needwood Basin; 5, East Midlands Shelf (South); 6, East Midlands Shelf (North); 7, Stafford Basin; 8, Cheshire Basin; 9, West Lancashire; 10, Carlisle Basin. After Howard *et al.* (2008). Contains 1:50 000 BGS DiGMap ©BGS UKRI and Ordnance Survey data © Crown Copyright and database rights 2020.

perpendicular to bedding and noted that the anisotropy was less for the siltier facies. Large infrastructure schemes (e.g. transit tunnels, ground source heating and cooling for commercial and public buildings) will require site-specific thermal properties that can only be derived from an onsite test such as a TRT. Databased thermal properties derived from sample testing, as presented here, are suitable for smaller infrastructure (e.g. domestic ground source heating and cooling) where the design can include some tolerance owing to the lack of site-specific values.

There are few thermal property data for the MMG in the literature. The Microgeneration Installation Standard for ground source heat pumps (MIS 3005 v5, Department of Energy and Climate Change 2017) lists a range of thermal conductivity for Marl of 1.5–3.5 W m^{-1} K^{-1} with a recommended value of 2.1 W m^{-1} K^{-1}. Quoted thermal conductivities for the MMG are 2.28 ± 0.33 W m^{-1} K^{-1} (Bloomer 1981), 1.88 ± 0.03 W m^{-1} K^{-1} (Rollin 1987) and 1.49–2.58 W m^{-1} K^{-1} (Banks *et al.* 2013) from *in situ* TRT. Given the lithological variation within the MMG, a mean value for the bulk MMG is unlikely to be representative of a site-specific effective thermal conductivity. The mean values quoted by Bloomer (1981) and Rollin (1987) are based on 41 and 225 laboratory measurements on samples respectively and assign a rock type of mudstone although a mix of lithologies are included. These data were collected as part of the 'Investigation of the geothermal energy of the UK' programme (Downing and Gray 1986) and are re-examined here. The data were collected for heat flow studies where the thermal conductivity perpendicular to bedding is required. Measurements were made either from core in a divided bar apparatus, where the natural moisture level was preserved, from rock chippings placed in a pill box placed in the divided bar apparatus or with a needle probe. In the case of the pill box measurements, corrections were applied to generate the bulk-rock thermal conductivity, but the random nature of the packing of the chippings in the pill box results in an averaged parallel or perpendicular to bedding thermal conductivity (Wheildon *et al.* 1985). Neither Bloomer (1981) nor Rollin (1987) gave a breakdown on the numbers of each type of measurement in their mean values. However, the data re-examined here are most probably the same as used by Rollin (1987) and of 220 measurements only 20 (9%) were by the pill box method. Hence, it is reasonable to assume that the majority were measurements of thermal conductivity perpendicular to bedding. The measurements of Banks *et al.* (2013) from TRT tests where heat flows radially from a borehole will be representative of horizontal thermal conductivity under field saturation conditions.

The individual measurements have been grouped by rock type, assignment to the revised lithostratigraphy (Howard *et al.* 2008) and provenance, and the results are shown in Table 3. Measured thermal conductivities from the Cleethorpes geothermal borehole for the East Midlands Shelf (north) are uniformly high and as noted by Busby (2018) there appears to be a systematic error in the thermal conductivities from this borehole, and hence they have been excluded. All of these data are thermal conductivities perpendicular to bedding with the exception of the bulk MMG value (1.95 W m^{-1} K^{-1}) in the Wessex Basin, which was from pill box measurements on chippings from the Marchwood borehole. The data in Table 3 show a range of values from 1.71 to 4.43 W m^{-1} K^{-1} with representative thermal conductivities for mudstone of 2.10 W m^{-1} K^{-1}, silty mudstone 1.87 W m^{-1} K^{-1}, siltstone 2.24 W m^{-1} K^{-1} and sandstone 3.31 W m^{-1} K^{-1}. There are no reported measurements of thermal diffusivity.

GeoEnergy Test Bed borehole

The British Geological Survey and the University of Nottingham have established a GeoEnergy Test Bed (GTB) research site to monitor CO_2 migration pathways in the shallow subsurface with advanced sensor technologies (Vincent *et al.* 2019). The GTB is located at the University of Nottingham's Sutton Bonington campus to the SW of Nottingham (52°49'51.44"N, 1°15'1.46"W; British National Grid [450600E, 326200N]). There are 11 boreholes on site, one of which was cored to its full depth of 282 m. This borehole penetrates a section of the East Midlands MMG comprising the Arden Sandstone Formation, the Sidmouth Mudstone Formation and the Tarporley Siltstone Formation. It therefore provides an opportunity to study in detail a section of the MMG and relate its thermal properties to structure and mineralogy. Twenty samples taken from the borehole core through this section were described and analysed to determine porosity, mineralogy and laboratory thermal properties.

Rock description

The upper two samples, SSK109105 and SSK109102, are from the Arden Sandstone Formation (see Table 4). The upper sample is a variably coloured, friable sandstone with near abundant, horizontal gypsum veining, whereas the lower sample is a light brown to red–brown sandy mudstone with hairline horizontal gypsum veins throughout. The majority of the cored sequence (14 samples) is from the Sidmouth Mudstone Formation. The samples from 21.7–46.0 m depth are brown to light brown and pale grey mudstones with near horizontal to horizontal gypsum veining throughout. The samples from 54.6–65.4 m depth are pale grey bleached fine sandstone with some poorly defined horizontal, fine paler bands and light red–brown to light grey–green (mottled) silty very fine to fine sandstones. Red–brown and pale brown sandy mudstones occur between 67.8 and 77.1 m depth and the sample at 85.6–85.7 m depth is a red–brown mudstone with pale grey–brown coloured wisps that show clear laminated structure. The remainder of the

Table 1. *Stratigraphic divisions of the Mercia Mudstone Group of England and Wales*

Group	Formation	Lithology	Rock types
Mercia Mudstone Group	Blue Anchor Formation (BAN)	Typically comprises pale green–grey, dolomitic silty mudstones and siltstones with thin arenaceous lenses and a few thin, commonly discontinuous beds of hard, dolomitic, pale yellowish grey, porcellanous mudstone and siltstone. Stratified bedrock	DSMDST, MDST, SLST, SLMDST, DOLO, GYPST
	Branscombe Mudstone Formation (BCMU)	Structureless mudstone and siltstone, red–brown with common grey–green reduction patches and spots. Gypsum/anhydrite, locally of economic importance, is common throughout in beds, nodules and veins. Sporadic thin beds of argillaceous sandstone and silty dolomite occur in the lower part of the formation. Stratified bedrock	MDST, SLST, GYPST, SDST
	Arden Sandstone Formation (AS)	Grey, green and purple mudstones interbedded with paler grey–green to buff coloured siltstones and fine- to medium-grained, varicoloured green, brown, buff, mauve sandstone. Stratified bedrock	MDST, SDST, SLST, CONG
	Sidmouth Mudstone Formation (SIM)	Mudstone and siltstone, red–brown with common grey–green reduction patches and spots. The mudstones are mostly structureless, with a blocky weathering habit, but intervals up to 15 m thick of interlaminated mudstone and siltstone occur within parts of the formation. Heterolithic units consisting of several thin beds of grey–green dolomitic siltstone and very fine-grained sandstone, interbedded with mudstone, occur at intervals throughout the formation. Units of halite up to 400 m thick are present at several stratigraphical levels in the thicker basinal sequences of the east Irish Sea, Cheshire, Staffordshire, Cleveland, Worcestershire, Somerset and Dorset, although they are most prevalent towards the top. Stratified bedrock	DSMDST, MDST, SLST, BREC, DSLST, HALI, DSDST, GYPST
	Tarporley Siltstone Formation (TPSF)	Interlaminated and interbedded siltstones, mudstones and sandstones in approximately equal proportions, trace conglomerate and limestone. Gypsum occurs sporadically in the mudstones as small nodules. Stratified bedrock	MDST, SDST, SLST, CONG, GYPST, LMST

The rock type descriptions are given in Table 2.

Table 2. *Rock types of the Mercia Mudstone Group*

Code	Description	Code	Description	Code	Description
DSMDST	Dolomitic silicate-mudstone	BREC	Breccia	DOLO	Dolostone
MDSD	Mudstone and sandstone	CONG	Conglomerate	GYPST	Gypsum-stone
MDSL	Mudstone, sandstone and limestone	DSDST	Dolomitic sandstone	HALI	Halite
MDSST	Muddy sandstone	DSLST	Dolomitic siltstone	LMMD	Mudmound limestone
MDST	Mudstone	SDSM	Sandstone, siltstone and mudstone	LMST	Limestone
		SDST	Sandstone		
		SLMDST	Silty mudstone		
		SLST	Siltstone		

Table 3. *Measured thermal conductivities of the MMG*

Wessex Basin		Worcester–Knowle Basin		East Midlands Shelf (south)		Cheshire Basin	
Code	TC ($W\,m^{-1}\,K^{-1}$)	Code	TC ($W\,m^{-1}\,K^{-1}$)	Code	TC ($W\,m^{-1}\,K^{-1}$)	Code	TC ($W\,m^{-1}\,K^{-1}$)
MMG-MDST	1.95 ± 0.38						
BAN-SLMDST	2.05*						
BCMU-LMMD	2.09 ± 0.16*	BCMU-MDST	2.81 ± 0.26	BCMU-MDST	1.88 ± 0.19		
BCMU-MDSL	2.34 ± 0.1*			BCMU-SLST	2.12		
BCMU-SLMDST	1.96 ± 0.41*						
		AS-SDST	3.17	AS-SDST	2.94		
SIM-SLMDST	1.72*	SIM-MDSD	2.63*	SIM-DSDST	2.76	SIM-MDST	1.89 ± 0.06*
		SIM-MDST	2.05 ± 0.1*	SIM-MDST	1.71 ± 0.14	SIM-SLMDST	1.69 ± 0.12*
		SIM-SLMDST	1.94 ± 0.12*	SIM-SDST	4.43		
		SIM-SLST	2.19 ± 0.31*	SIM-SLST	2.40 ± 0.41		
				TPSF-SDST	2.70 ± 0.37		

*Data source is Wheildon *et al*. (1985). All other values are held by the BGS.
Errors were calculated with Peter's formula. Values with no error are single measurements. Code is a combination of the lithostratigraphy and rock type classification.

Sidmouth Mudstone Formation is arenaceous with silty very fine sandstones and massive very silty, clayey very fine-grained sandstone with gypsum veining increasing towards the base of the Formation. The upper sample in the Tarporley Siltstone Formation (131.9–132.0 m depth) is a massive red–brown very silty very fine sandstone. The sample from 140.4–140.6 m depth interval is a more variable sample comprising muddy clasts in a mud clast rich bed with no gypsum veining. The final two samples at the base of the

Table 4. *Mineralogical compositions of the GTB core samples (presented as volume percentages of the whole rock), effective porosity and rock classifications determined from the rock descriptions*

SSK number	Depth (m)	Volume % of whole rock												Effective porosity	Rock type classification
		Quartz	Plagioclase	K-feldspar	Mica (excl illite)	Illite	Smectite	Chlorite (incl. corrensite)	Calcite	Dolomite	Hematite	Gypsum	Anhydrite		
Arden Sst Fm															
109105	9.3–9.4	17.8	0.9	<0.5	3.7	4.2	4.2	0.8	1.1	8.3	<0.5	29.1	n.d.	29.7	SDST
109102	14.4–14.5	9.5	1.2	<0.5	3.6	3.6	7.6	1.7	0.7	9.6	<0.5	24.2	n.d.	37.7	MDSST
Sidmouth Mdst Fm															
109103	21.7–21.8	18.0	2.3	<0.5	22.9	3.6	n.d.	2.9	n.d.	4.3	n.d.	13.3	n.d.	32.3	MDST
109104	30.3–30.5	72.5	1.8	<0.5	7.9	0.9	n.d.	0.7	n.d.	3.2	<0.5	2.5	n.d.	10.2	MDSST
109080	37.1–37.5	21.5	2.8	1.6	6.9	6.8	14.7	5.6	n.d.	6.7	<0.5	4.1	n.d.	29.0	MDST
109081	45.7–46.0	35.2	1.9	1.9	5.4	12.1	n.d.	7.6	n.d.	2.4	<0.5	5.6	n.d.	27.8	MDSST
109082	54.6–54.7	60.8	n.d.	5.4	1.4	<0.5	n.d.	<0.5	n.d.	3.3	n.d.	3.7	20.5	4.2	SDST
109083	65.3–65.4	43.2	3.8	5.7	7.4	7.1	n.d.	1.5	n.d.	16.3	n.d.	n.d.	n.d.	15.0	SDST
109084	68.0–68.1	8.1	0.6	3.9	2.9	4.5	n.d.	<0.5	n.d.	46.4	n.d.	15.6	n.d.	17.6	MDSST
109085	76.8–77.1	13.4	<0.5	5.4	3.9	3.7	n.d.	1.9	n.d.	43.7	n.d.	12.6	n.d.	15.1	MDSST
109086	85.6–85.7	37.1	<0.5	8.5	4.5	7.3	n.d.	1.4	n.d.	23.4	<0.5	1.8	n.d.	15.8	MDST
109087	93.9–94.0	30.9	<0.5	7.1	6.0	6.1	n.d.	1.8	n.d.	19.9	<0.5	9.8	n.d.	18.2	SDST
109088	100.7–100.8	26.8	<0.5	5.6	3.6	7.8	n.d.	2.0	n.d.	32.5	<0.5	3.5	n.d.	17.7	SDST
109089	108.7–108.8	41.4	0.8	5.2	6.0	7.7	n.d.	1.4	n.d.	18.0	<0.5	2.1	n.d.	17.1	SDSM
109096	116.4–116.5	45.6	<0.5	6.4	9.8	4.7	n.d.	4.6	n.d.	12.7	n.d.	2.0	n.d.	13.9	SDST
109097	124.4–124.6	54.2	0.8	6.4	6.4	6.6	n.d.	1.0	n.d.	7.9	<0.5	1.8	n.d.	14.9	SDSM
Tarporley Slst Fm															
109098	131.9–132.0	47.7	0.7	3.7	7.8	6.3	n.d.	0.7	n.d.	10.6	<0.5	5.7	n.d.	16.6	SLST
109099	140.4–140.6	39.9	0.7	7.1	6.9	12.8	n.d.	0.7	n.d.	15.6	<0.5	<0.5	n.d.	15.9	MDST
109100	148.3–148.4	80.5	n.d.	0.5	n.d.	0.6	<0.5	n.d.	n.d.	<0.5	<0.5	6.2	n.d.	11.6	SDST
109101	155.8–156.0	47.9	<0.5	5.2	7.9	10.3	n.d.	1.5	n.d.	10.9	<0.5	0.7	n.d.	15.3	SLST

n.d., not detected.

cored section comprise red–brown and grey–brown silty very fine sandstone and a mottled grey–green to red–brown–grey fine siltstone with some well-developed horizontal laminations, possibly current ripples.

Porosity estimations

The samples were saturated with water under vacuum before drying at 100°C for 16 h. The weight difference before and after drying was used to estimate the effective porosity. Such estimates will have an element of error owing to water adsorbed onto grain or clay mineral surfaces, particularly for the clay-rich samples. Additionally, the rocks have a fine grain size, are heavily compacted and have a high clay content, which means that the diameters of pore throats, which connect pores, are likely to be small and also infilled with impermeable clay material, limiting the effectiveness of the saturating and drying process.

X-ray diffraction analysis

The mineralogy of the samples was determined using a combination of whole-rock and <2 μm X-ray diffraction (XRD) analyses.

Sample preparation

The core samples were dried at 55°C overnight and jaw-crushed. Half of the jaw-crushed material was representatively subsampled and ball-milled for whole-rock XRD analyses.

To provide a finer and uniform particle size for powder XRD analysis, a portion of the ball-milled sample was micronized under distilled water for 10 min with 10% corundum and dried at 55°C. The samples were then spray-dried following the method and apparatus described by Hillier (1999). The spray-dried material was then front-loaded into a standard stainless steel sample holder for analysis.

To separate a fine fraction for clay mineral XRD analysis, further portions of the jaw-crushed material were dispersed in distilled water using a reciprocal shaker combined with ultrasound treatment and then wet-sieved on 63 μm mesh. The coarse (>63 μm) material was collected and dried in an oven at 55°C ('sand'). The <63 μm material was placed in a measuring cylinder with a few drops of 0.1M Calgon solution to prevent clay flocculation and shaken. The suspension was left to settle and after a time period determined from Stokes' Law, a nominal <2 μm fraction was removed to a stock beaker. The cylinders were then topped up with distilled water, shaken, and the suspensions allowed to stand for a similar time period before a further <2 μm fraction was removed and added to the stock beaker. The process was repeated for a third extraction before the <2 μm material was then dried at 55°C and stored in glass vials ('clay'). The remaining 2–63 μm was also dried at 55°C and stored in glass vials ('silt').

Approximately 100 mg of the dried <2 μm material was then re-suspended in a minimum of distilled water and pipetted onto a ceramic tile in a vacuum apparatus to produce an oriented mount. The mounts were Ca-saturated using 0.1M $CaCl_2.6H_2O$ solution, washed twice to remove excess reagent and allowed to air-dry overnight.

The preparation of <2 μm material for XRD analysis therefore also provided a crude particle size analysis for the samples. However, these particle size distributions (PSD) data should be regarded with caution as the samples were not fully disaggregated and therefore the proportions of 'sand'- and 'silt'-grade material are almost certainly overestimates and the quantity of 'clay'-grade material is therefore underestimated.

Analysis

XRD analyses were carried out using a PANalytical X'Pert Pro series diffractometer equipped with a cobalt-target tube and X'Celerator detector and operated at 45 kV and 40 mA.

The spray-dried powder mounts were scanned from 4.5 to 85°2θ at 2.06°2θ min^{-1}. Diffraction data were analysed using PANalytical X'Pert HighScore Plus version 4.8 software coupled to the latest version of the International Centre for Diffraction Data (ICDD) database.

The <2 μm oriented mounts were scanned from 2 to 40°2θ at 1.02°2θ min^{-1} after air-drying, after glycol-solvation and after heating to 550°C for 2 h.

Whole-rock quantification

Following identification of the mineral species present in the sample, phase quantification was achieved using the Rietveld refinement technique (e.g. Snyder & Bish 1989) using PANalytical HighScore Plus software. Errors for the quoted mineral concentrations are typically ±1% for concentrations >50 wt%, ±5% for concentrations 10–50 wt% and ±10% for concentrations <10 wt% (e.g. Kemp *et al.* 2016*b*). Where a phase was detected but its concentration was indicated to be below 0.5%, it is assigned a value of <0.5%, as the error associated with quantification at such low levels becomes too large.

XRD profile modelling

To gain further information about the nature of the clay minerals present in the sample, modelling of the XRD profiles was carried out using Newmod II™ (Reynolds & Reynolds 2013) software following the method summarized by Kemp *et al.* (2016*a*). Modelling was also used to assess the relative proportions of clay minerals present in the <2 μm fraction by comparison of sample XRD traces with Newmod II™ modelled profiles following the method outlined by Moore & Reynolds (1997).

Thermal properties measurements

Laboratory measurements of thermal conductivity and diffusivity of the GTB samples were undertaken by the Geological Survey of Belgium (GSB). At each of the 20 sampling points down the GTB core, two samples were taken. One half of the sample was used for the XRD analysis, and the other was cut into a smooth-sided square block of dimensions 40 × 40 × 10 mm. As a result of the sampling technique the samples were not oriented and therefore it is not known if the thermal properties measurements were parallel or perpendicular to bedding. The thermal properties measurements were made in Belgium with the high-resolution optical thermal conductivity scanning method (Popov *et al.* 1999, 2012). This is a high-precision non-contact measurement that optically scans the sample's surface with a focused, mobile and continuously operated heat source in combination with two infrared temperature sensors. After warming up the instrument, the sensors were calibrated with a reference sample. The measurements were made on a 2 cm wide black mark made on the plane surface of each sample. All the measurements were repeated three times from which mean values were calculated. The device operates in two modes: thermal conductivity alone, or a combined mode of thermal conductivity and thermal diffusivity. Measurements were made initially on unsaturated samples and then repeated after saturation in a vacuum desiccator by demineralized water for 5–10 days. The results quoted here are only for saturated samples and the thermal conductivity results are from the thermal 'conductivity alone' mode, whereas the thermal diffusivity results are from the combined mode. Sample SSK109089 was fractured and broken resulting in inconsistent results, especially between the unsaturated and saturated states, and so has been discounted. The specific heat capacity by mass was calculated as the saturated density was measured during the porosity

Table 5. *Measured thermal conductivities, thermal diffusivities, saturated densities and derived specific heats for the GTB core samples*

SSK number	Thermal conductivity ($W\,m^{-1}\,K^{-1}$)	Thermal diffusivity ($\times 10^{-6}\,m^2\,s^{-1}$)	Saturated density ($kg\,m^{-3}$)	Specific heat capacity by mass ($J\,K^{-1}\,kg^{-1}$)	Specific heat capacity by volume ($MJ\,m^{-3}\,K^{-1}$)
Arden Sst Fm					
109105	1.64 ± 0.01	0.64 ± 0.03	2315	1109	2.57
109102	1.67 ± 0.02	0.79 ± 0.08	2143	993	2.13
Sidmouth Mdst Fm					
109103	1.65 ± 0.03	0.63 ± 0.05	2227	1179	2.63
109104	3.10 ± 0.05	1.43 ± 0.07	2497	867	2.17
109080	1.79 ± 0.02	0.64 ± 0.01	2236	1254	2.80
109081	2.07 ± 0.01	0.65 ± 0.07	2235	1426	3.19
109082	5.60 ± 0.15	3.07 ± 0.29	2653	688	1.82
109083	2.32 ± 0.01	1.47 ± 0.05	2454	643	1.58
109084	2.85 ± 0.03	1.12 ± 0.07	2499	1019	2.55
109085	2.82 ± 0.03	1.70 ± 0.05	2473	669	1.65
109086	2.65 ± 0.02	1.16 ± 0.01	2443	940	2.30
109087	2.18 ± 0.03	0.95 ± 0.02	2575	891	2.29
109088	2.50 ± 0.01	1.48 ± 0.15	2643	642	1.70
109089	n.d.	n.d.	n.d.	n.d.	n.d.
109096	2.44 ± 0.04	1.06 ± 0.03	2530	910	2.30
109097	2.85 ± 0.03	1.31 ± 0.16	2437	894	2.18
Tarporley Slst Fm					
109098	2.60 ± 0.04	0.96 ± 0.09	2610	1034	2.70
109099	2.31 ± 0.33	1.56 ± 0.18	2636	563	1.48
109100	4.14 ± 0.02	2.11 ± 0.09	2585	760	1.96
109101	2.22 ± 0.02	1.03 ± 0.0	2474	871	2.16

n.d., not detected. Thermal conductivities and diffusivities were determined from three measurements and errors have been calculated with Peter's formula.

measurement. It is given by

$$S_c = \frac{\lambda}{\alpha\rho}$$

where S_c is the specific heat by mass ($J\,K^{-1}\,kg^{-1}$), λ is thermal conductivity ($W\,m^{-1}\,K^{-1}$), ρ is the saturated density ($kg\,m^{-3}$) and α is the thermal diffusivity ($m^2\,s^{-1}$). The specific heat capacity by volume has also been calculated, as it is the product of the specific heat by mass and the density.

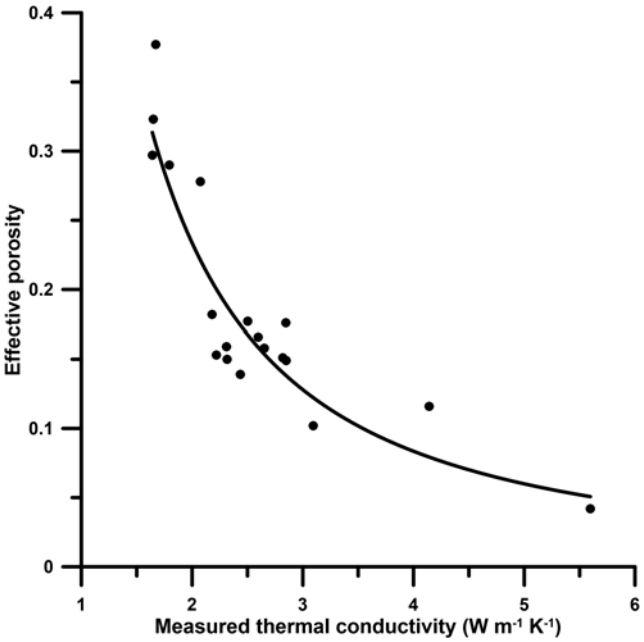

Fig. 2. Plot of effective porosity versus measured thermal conductivity. The data display a distinctly non-linear relationship, which has been approximated by a power fit of the form $Y = aX^b$.

Results of the GTB core analyses

Porosity and XRD mineralogical results are summarized in Table 4. Mineral contents were measured as weight percentages of the sample, converted to volume percentages of the sample and finally converted to volume percentages of the rock, taking into consideration the effective porosity. The proportions of illite were measured in the <2 μm material analyses where illite is the dominant clay mineral. Quartz is the most abundant mineral followed by dolomite and gypsum. Measured thermal conductivities, thermal diffusivities, saturated densities and derived specific heats are given in Table 5. Thermal conductivity has a range from 1.64 to 5.6 $W\,m^{-1}\,K^{-1}$. The highest thermal conductivities correlate with samples with high percentages of high thermal conductivity minerals and/or low porosities. A high porosity will lower the thermal conductivity as the pore space is filled by low thermal conductivity water. Sample SSK109082, which has the highest thermal conductivity of 5.6 $W\,m^{-1}\,K^{-1}$, contains 59.7% quartz and 22.1% anhydrite (mineral thermal conductivities of 7.69 $W\,m^{-1}\,K^{-1}$ and 4.76 $W\,m^{-1}\,K^{-1}$ respectively) and a low porosity of 4.2%. Sample SSK109100 has the second highest thermal conductivity of 4.14 $W\,m^{-1}\,K^{-1}$ and has the highest quartz content of 81.1%, but a higher porosity of 11.6%. The Arden Sandstone samples (SSK109105 and SSK109102) both have relatively low thermal conductivities corresponding to low quartz content, high gypsum content (thermal conductivity 2.9 $W\,m^{-1}\,K^{-1}$) and high porosities. Secondary mineralization in the form of veins and nodules is common in the MMG and where it occurs it could have a significant influence on the thermal conductivity. Gypsum is also likely to occur as a cement, connecting or bridging the higher conducting quartz grains, which would have the overall effect of lowering the thermal conductivity of the rock.

From the repeated measurements on the GTB core samples there is an overall measurement error of ±2% in thermal conductivity and ±6% in thermal diffusivity. Uncertainty will be greater owing to microstructural features such as bedding and when translating measured sample values to the rock mass where macrostructural features may have an effect.

Table 6. *Thermal conductivities assigned to the minerals and pore fluid in the geometric mean modelling*

Model component	Thermal conductivity ($W\,m^{-1}\,K^{-1}$)	Reference
Hematite	11.28	Clauser and Huenges (1995)
Quartz	7.69	Clauser and Huenges (1995)
Dolomite	5.51	Clauser and Huenges (1995)
Anhydrite	4.76	Horai (1971)
Calcite	3.59	Clauser and Huenges (1995)
Chlorite	3.26	Brigaud and Vasseur (1989)
Gypsum	2.9	Brigaud and Vasseur (1989)
K-feldspar	2.45	Horai (1971)
Mica (excluding illite)	2.2	Horai (1971)
Smectite	1.88	Brigaud and Vasseur (1989)
Illite	1.85	Brigaud and Vasseur (1989)
Plagioclase	1.84	Horai (1971)
Water	0.6	Ozbek and Phillips (1979)

For the sizing of a GSHP closed-loop borehole, it is the average thermal conductivity of the strata over the length of the borehole that is required. For the GTB core, it has been assumed that each sample is representative of an equal thickness layer within each formation. This translates to layer thicknesses of 4.5 m within the Arden Sandstone, 7.9 m within the Sidmouth Mudstone and 7 m within the Tarporley Siltstone. Because heat will be flowing horizontally into the borehole an arithmetic mean, weighted by the layer thicknesses, has been calculated as 2.63 $W\,m^{-1}\,K^{-1}$. This is higher than might be expected for a rock referred to as a mudstone, but reflects the arenaceous nature of the sequence in the GTB core. From four TRT measurements, Banks *et al.* (2013) quoted an upper MMG thermal conductivity of 2.58 $W\,m^{-1}\,K^{-1}$, a value compatible with that from the GTB core.

Figure 2 shows a plot of increasing thermal conductivity with decreasing effective porosity, which displays a non-linear relationship. The thermal diffusivities show a range of 0.63–3.07 × 10^{-6} $m^2\,s^{-1}$. There are no published data on measured thermal diffusivities of the MMG, but these values are comparable with those reported by Labus and Labus (2018) on fine-grained sedimentary rocks. The specific heats by mass range from 563 to 1426 $J\,K^{-1}\,kg^{-1}$ and the specific heats by volume range from 1.48 to 3.19 $MJ\,m^{-3}\,K^{-1}$.

Estimations of thermal conductivity from mineral content

The number of thermal conductivity determinations can be increased by applying a modelling approach when the mineral content of the rock is known. This has been applied to two sets of MMG samples reported in the literature by Kemp and Hards (1999) and Armitage *et al.* (2013). However, because the GTB site has yielded both laboratory determinations of thermal conductivity and mineral content, the modelling procedure has been tested for its effectiveness for Mercia Mudstone before being applied to the data of Kemp and Hards (1999) and Armitage *et al.* (2013).

The modelling was based on multi-component mixture models, as summarized by Clauser (2006). Owing to their well-defined compositions, the thermal conductivities of individual minerals show a much smaller variance than those of rocks and can be combined with the thermal conductivities of the saturating fluids to estimate the thermal conductivity of the rock. Fuchs *et al.* (2013) examined the goodness-of-fit between measured and modelled thermal conductivities for 1147 samples of sedimentary rocks (sandstone, mudstone, limestone and dolomite). They compared five mixture models comprising the geometric mean, the arithmetic mean, the harmonic mean, the Hashin and Shtrikman mean and the effective-medium theory mean. They considered only a two-component system comprising rock matrix and pores, but concluded that the geometric mean gave the best results. Hence, the geometric mean model has been applied here. The geometric mean thermal

Table 7. *Calculated geometric mean thermal conductivities, GSB measured saturated thermal conductivities, deviation between the measured and calculated thermal conductivities and the corrected calculated geometric mean thermal conductivities after applying a correction factor based on the lithotype*

SSK number	Geometric mean thermal conductivity ($W\,m^{-1}\,K^{-1}$)	Measured thermal conductivity ($W\,m^{-1}\,K^{-1}$)	Deviation measured to calculated thermal conductivity ($W\,m^{-1}\,K^{-1}$)	Lithotype	Corrected geometric mean thermal conductivity ($W\,m^{-1}\,K^{-1}$)
Arden Sst Fm					
109105	2.18	1.64 ± 0.01	−0.53	Sandstone	1.22
109102	1.77	1.67 ± 0.02	−0.09	Mudstone	1.13
Sidmouth Mdst Fm					
109103	1.96	1.65 ± 0.03	−0.31	Mudstone	1.33
109104	4.95	3.10 ± 0.05	−1.86	Mudstone	4.32
109080	2.10	1.79 ± 0.02	−0.30	Mudstone	1.46
109081	2.50	2.07 ± 0.01	−0.42	Mudstone	1.86
109082	5.47	5.60 ± 0.15	0.13	Sandstone	4.51
109083	3.58	2.32 ± 0.01	−1.27	Sandstone	2.62
109084	3.09	2.85 ± 0.03	−0.24	Mudstone	2.45
109085	3.33	2.82 ± 0.03	−0.51	Mudstone	2.69
109086	3.56	2.65 ± 0.02	−0.91	Mudstone	2.93
109087	3.17	2.18 ± 0.03	−0.99	Sandstone	2.21
109088	3.33	2.50 ± 0.01	−0.83	Sandstone	2.37
109089	n.d.	n.d.	n.d.	Sandstone	n.d.
109096	3.73	2.44 ± 0.04	−1.30	Sandstone	2.77
109097	3.86	2.85 ± 0.03	−1.01	Sandstone	2.90
Tarporley Slst Fm					
109098	3.60	2.60 ± 0.04	−1.00	Sandstone	2.64
109099	3.38	2.31 ± 0.33	−1.06	Mudstone	2.74
109100	5.29	4.14 ± 0.02	−1.15	Sandstone	4.33
109101	3.62	2.22 ± 0.02	−1.40	Sandstone	2.66

n.d., not detected.

conductivity of an n-component system is the product of the thermal conductivity of each component raised to the power of its volume fractional component; that is,

$$\lambda_b = \prod_{i=1}^{n} \lambda_i^{\varphi_i}$$

where λ_b is the mean bulk thermal conductivity, λ_i is the thermal conductivity of the ith component and φ_i is the volume fractional proportion of the ith component.

The thermal conductivities of the model components are listed in Table 6. It has been assumed that the samples are fully saturated with water. The calculated thermal conductivities are shown in Table 7.

Also listed in Table 7 are the measured thermal conductivities and the deviation between the measured and calculated thermal conductivities, and Figure 3 is a plot of measured versus calculated thermal conductivity. Except for one sample, the geometric mean calculated thermal conductivities are higher than the measured values, indicating an overestimation of mudstone thermal conductivity with the geometric mean model, an observation noted by Midttømme *et al.* (1998). A simple correction factor has been calculated as the average absolute deviation between the calculated and measured thermal conductivities. Correction factors for the mudstone and sandstone lithotypes have been calculated separately, where the lithotype is based on the rock description. The correction factors are 0.63 W m^{-1} K^{-1} for mudstone and 0.96 W m^{-1} K^{-1} for sandstone and these values were subtracted from the calculated thermal conductivities. The corrected values are listed in Table 7 and shown in Figure 3.

Kemp and Hards (1999) reported the results of mineralogical, petrological and surface area analyses from five samples taken from shallow boreholes at Northgates, Leicester. The samples were described as predominantly mudstone with some silty mudstone and siltstone. The samples are from the Sidmouth Mudstone Formation and, from the clay mineral assemblages, are representative of an interval that spans the junction between the Edwalton and Cropwell

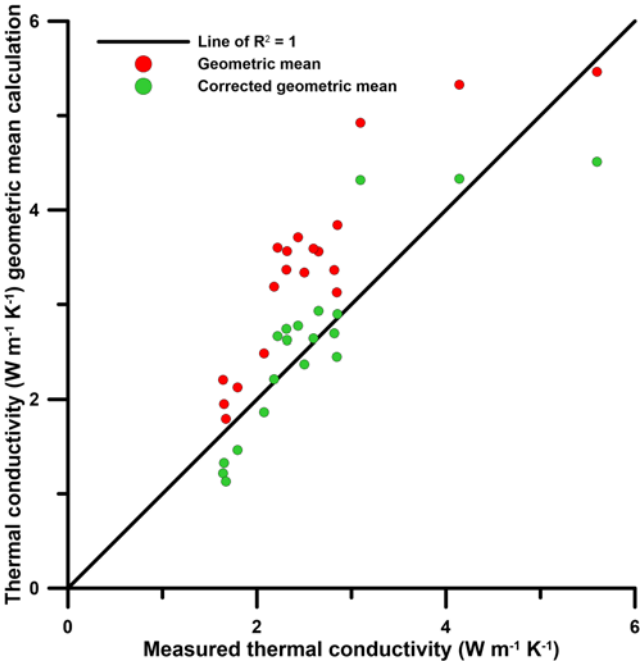

Fig. 3. Plot of calculated geometric mean thermal conductivity versus measured thermal conductivity (red symbols). The green symbols refer to the geometric mean thermal conductivity after application of a correction factor.

Table 8. *Mineral compositions (presented as volume percentages of the whole rock) and effective porosity of the samples reported by Kemp and Hards (1999) and Armitage et al. (2013)*

Sample number	Depth (m)	Volume % of whole rock										Effective porosity
		Quartz	Plagioclase	K-feldspar	Mica	Illite	Smectite	Chlorite	Calcite	Dolomite	Hematite	Gypsum	
Sidmouth Mdst Fm (Kemp and Hards 1999)													
Borehole 2/2	8.0	21.7	0.9	7.5	7.5		17.7	0.9	13.2	9.3	0.5	n.d.	21.0
Borehole 2/6	8.5–10.0	30.1	1.7	8.0	6.3		11.9	0.8	16.8	3.2	0.0	n.d.	21.0
Borehole 2/8	8.0	32.8	1.8	8.3	8.2		13.3	0.8	3.5	9.9	0.5	n.d.	21.0
Borehole 2/10	8.25–9.0	31.7	2.6	8.9	7.1		13.8	0.8	0.8	12.8	0.4	n.d.	21.0
Borehole 2/13	9.1–10.3	15.0	0.8	8.6	5.4		26.9	0.8	15.5	5.5	0.4	n.d.	21.0
Sidmouth Mdst Fm (Armitage et al. 2013)													
M1	300.0	29.4	1.8	14.7		36.9		5.3	3.1	1.3	n.d.	0.0	7.4
M2	300.4	39.6	1.5	10.3		14.0		3.9	0.4	7.4	n.d.	12.4	10.3
M3	301.5	29.1	2.1	10.4		16.0		3.7	0.2	11.1	n.d.	16.9	10.7
M4	302.6	39.7	0.5	7.0		30.7		4.2	0.2	8.4	n.d.	0.1	9.1
M5	307.5	43.1	0.1	7.9		33.5		4.4	0.1	1.3	n.d.	0.0	9.7
M6	309.3	59.3	0.9	5.9		3.8		1.4	0.9	3.2	n.d.	15.1	9.5

n.d., not detected.

Table 9. *Results of the geometric mean thermal conductivity modelling for the samples reported by Kemp and Hards (1999) and Armitage et al. (2013)*

Sample number	Rock type	Geometric mean thermal conductivity (W m^{-1} K^{-1})	Correction factor applied	Corrected geometric mean thermal conductivity (W m^{-1} K^{-1})
Sidmouth Mdst Fm (Kemp and Hards 1999)				
Borehole 2/2	MDST	2.49	−0.63	1.86
Borehole 2/6	SDSM	2.67	−0.96	1.71
Borehole 2/8	MDST	2.76	−0.63	2.13
Borehole 2/10	MDST	2.76	−0.63	2.13
Borehole 2/13	SLMDST	2.21	−0.63	1.57
Sidmouth Mdst Fm (Armitage et al. 2013)				
M1	SLMDST	2.82	−0.63	2.19
M2	SLST	3.13	−0.96	2.17
M3	SLMDST	2.74	−0.96	1.78
M4	SLMDST	3.33	−0.63	2.70
M5	SLMDST	3.22	−0.96	2.26
M6	SDST	3.88	−0.96	2.92

Bishop members. Kemp and Hards (1999) did not measure effective porosity and so the average value of the GTB mudstone samples (21%) has been used. The mineral compositions of the samples are shown in Table 8. Armitage *et al.* (2013) studied six samples from depths between 300 and 310 m from the Willow Farm borehole in the East Midlands near Nottingham (52°51'27.23"N, 0°52'52.00"W; [475434E, 329483N]). The samples vary from muddy siltstones to silty to very fine-grained sandstones and are also from the Sidmouth Mudstone Formation. The mineral compositions are also listed in Table 8. Thermal conductivities for these 11 samples have been calculated with the geometric mean model and corrected using the correction factors estimated above and the results are listed in Table 9. The range of the corrected geometric mean thermal conductivity values is 1.57 W m^{-1} K^{-1} (silty mudstone) to 2.92 W m^{-1} K^{-1} (sandstone).

Discussion

The measured thermal conductivities from the GTB core have been incorporated with the data in Table 3 to create a revised set of thermal conductivities for the East Midlands shelf (south) MMG, and this is shown in Table 10. From a consideration of all the measured data (Tables 3 and 10), there is a range in thermal conductivity of 1.67–3.24 W m^{-1} K^{-1} for the MMG. The lower values are for the mudstones, 1.67–2.81 W m^{-1} K^{-1}. The siltstones range from 2.12 to 2.41 W m^{-1} K^{-1} and the sandstones from 2.3 to 3.24 W m^{-1} K^{-1}.

The uncorrected thermal conductivities calculated from the mineral content are uniformly higher than the measured values for the GTB core. Midttømme *et al.* (1998) in a study of mudstones noted that the grain size distribution may be a factor in the determination of thermal conductivity. Low measured thermal conductivities correlated with rocks with a high clay fraction, whereas rocks with a high sand fraction were associated with high thermal conductivities. Figure 4 is a plot of the clay fraction (<2 μm) and the sand fraction (>63 μm) of the GTB samples plotted against the measured thermal conductivity. Trends of higher measured thermal conductivity associated with a higher sand fraction and lower measured thermal conductivity associated with a higher clay fraction are apparent, suggesting that a model that does not take into account particle size fractions may not be suitable for predicting the thermal conductivity of the MMG.

There are other considerations for the mismatch between measured and modelled thermal conductivity. First, the model does not take into account anisotropy. Mudstones often display a different thermal conductivity parallel and perpendicular to bedding (Bloomer 1981). In the measurements from the GTB core no account was taken of anisotropy and so it is not possible to quantify the effect of anisotropy on the modelling. Second, the model considers only porosity that is assumed to be saturated, although for mudstones there may be water adsorbed onto grain or clay mineral surfaces that is not accounted for in the model.

From the GTB results, correction factors for the mudstone and sandstone lithotypes were applied to the calculations from Kemp and Hards (1999) and Armitage *et al.* (2013). These data have not been incorporated in the summary in Table 10 owing to the

Table 10. *Revised measured thermal conductivities for the East Midlands Shelf (south) MMG, incorporating the measured thermal conductivities from the GTB core*

Code	TC (W m^{-1} K^{-1})
BCMU-MDST	1.88 ± 0.19
BCMU-SLST	2.12
AS-MDSST	1.67
AS-SDST	2.3 ± 0.81
SIM-DSDST	2.76
SIM-MDSST	2.71 ± 0.23
SIM-MDST	1.81 ± 0.39
SIM-SDSM	2.85
SIM-SDST	3.24 ± 0.66
SIM-SLST	2.40 ± 0.41
TPSF-MDST	2.31
TPSF-SDST	2.99 ± 0.47
TPSF-SLST	2.41 ± 0.24

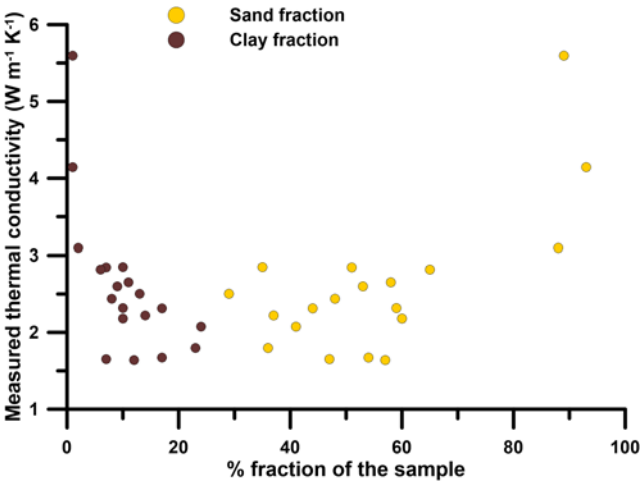

Fig. 4. Plot of measured thermal conductivity versus the sand and clay fractions of the GTB core samples.

limitations in the geometric mean model. However, the corrected thermal conductivities do fall within the ranges observed for measured values. Hence, if only mineralogical information is available, calculated thermal conductivities based on corrected geometric mean modelling may be valid for a first estimate of MMG thermal conductivity.

Conclusions

Previous publications that have included the thermal properties of the Mercia Mudstone Group have treated it as a single rock type and generated an average thermal conductivity from measurements on multiple lithologies. Data from the literature and new thermal conductivity and diffusivity measurements on a cored section of the MMG from the GTB borehole have been combined to generate revised thermal properties for the MMG. These indicate a total range in saturated vertical thermal conductivity of 1.67–3.24 W m^{-1} K^{-1}, comprising 1.67–2.81 W m^{-1} K^{-1} for mudstones, 2.12–2.41 W m^{-1} K^{-1} for siltstones and 2.30–3.24 W m^{-1} K^{-1} for sandstones. There is still limited availability of data and it is therefore not possible to draw conclusions about the variation of MMG thermal properties between the regions. However, the measured thermal diffusivities, ranging from 0.63 to 3.07×10^{-6} m^2 s^{-1}, are amongst the first published values for the MMG. These data are all from measurements on samples and there will be uncertainty when considering the thermal properties of the rock mass owing to micro- and macrostructural features. However, these data will improve the design of smaller infrastructure, such as domestic-scale ground source heat and cooling, where it is not possible to obtain site-specific thermal properties. Larger infrastructure schemes, where site-specific properties are required, should include a TRT in the design process.

The total number of estimations of thermal conductivity has been increased with geometric mean modelling based on mineralogy. Comparison with the measured thermal conductivities from the GTB core indicates that the modelled data are overestimated. Correction factors of 0.63 W m^{-1} K^{-1} for mudstone lithotypes and 0.96 W m^{-1} K^{-1} for sandstone lithotypes can be applied to allow a first estimate of MMG thermal conductivities when only mineralogical data are available.

Acknowledgements O. Wakefield is thanked for his initial logging of the core from the GTB borehole. D.P., J.B., S.K. and I.M. publish with the permission of the Executive Director, British Geological Survey (UKRI).

Author contributions **JPB**: conceptualization (lead), project administration (supporting), writing – original draft (lead), writing – review & editing (equal); **DP**: data curation (lead), formal analysis (equal), writing – original draft (equal), writing – review & editing (supporting); **SJK**: formal analysis (lead), methodology (equal), writing – original draft (equal), writing – review & editing (equal); **EP**: formal analysis (lead), writing – original draft (supporting); **IM**: formal analysis (supporting).

Funding The research was funded by the British Geological Survey (UKRI).

Data availability statement All data generated or analysed during this study are included in this published article.

Scientific editing by Jonathan Smith; David Birks

References

Armitage, P.J., Worden, R.H., Faulkner, D.R., Aplin, A.C., Butcher, A.R. and Espie, A.A. 2013. Mercia Mudstone Formation caprock to carbon capture and storage sites: petrology and petrophysical characteristics. *Journal of the Geological Society, London*, **170**, 119–132, https://doi.org/10.1144/jgs2012-049

Banks, D., Withers, J.G., Cashmore, G. and Dimelow, C. 2013. An overview of the results of 61 *in situ* thermal response tests in the UK. *Quarterly Journal of Engineering Geology and Hydrogeology*, **46**, 281–291, https://doi.org/10.1144/qjegh2013-017

Bloomer, J.R. 1981. Thermal conductivities of mudrocks in the United Kingdom. *Quarterly Journal of Engineering Geology*, **14**, 357–362, https://doi.org/10.1144/GSL.QJEG.1981.014.04.12

Brigaud, F. and Vasseur, G. 1989. Mineralogy, porosity and fluid control on thermal conductivity of sedimentary rocks. *Geophysical Journal*, **98**, 525–542, https://doi.org/10.1111/j.1365-246X.1989.tb02287.x

Busby, J. 2018. A modelling study of the variation of thermal conductivity of the English Chalk. *Quarterly Journal of Engineering Geology and Hydrogeology*, **51**, 417–423, https://doi.org/10.1144/qjegh2017-127

Clauser, C. 2006. Geothermal energy. *In*: Heinloth, K. (ed.) *Landolt-Börnstein, Group VIII: 'Advanced Materials and Technologies', Vol. 3 'Energy Technologies', Subvol. C 'Renewable Energies'*. Springer, Heidelberg, 480–595.

Clauser, C. and Huenges, E. 1995. Thermal conductivity of rocks and minerals. *In*: Ahrens, T.J. (ed.) *Rock Physics and Phase Relations: A Handbook of Physical Constants*. American Geophysical Union, Washington, DC, 105–126.

Department of Energy and Climate Change 2017. *Microgeneration Installation Standard: MIS 3005 v5. Requirements for MCS contractors undertaking the supply, design, installation, set to work, commissioning and handover of microgeneration heat pump systems Issue 5.0*. Department of Energy and Climate Change, https://mcscertified.com/wp-content/uploads/2019/08/MIS-3005.pdf

Downing, R.A. and Gray, D.A. 1986. Geothermal resources of the United Kingdom. *Journal of the Geological Society, London*, **143**, 499–507, https://doi.org/10.1144/gsjgs.143.3.0499

Fuchs, S., Schütz, F., Förster, H.-J. and Förster, A. 2013. Evaluation of common mixing models for calculating bulk thermal conductivity of sedimentary rocks: Correction charts and new conversion equations. *Geothermics*, **47**, 40–52, https://doi.org/10.1016/j.geothermics.2013.02.002

Hillier, S. 1999. Use of an air-brush to spray dry samples for X-ray powder diffraction. *Clay Minerals*, **34**, 127–135, https://doi.org/10.1180/000985599545984

Horai, K. 1971. Thermal conductivity of rock forming minerals. *Journal of Geophysical Research*, **76**, 1278–1308, https://doi.org/10.1029/JB076i005p01278

Howard, A.S., Warrington, G., Ambrose, K. and Rees, J.G. 2008. *A formational framework for the Mercia Mudstone Group (Triassic) of England and Wales*. British Geological Survey Research Report, **RR/08/04**.

Kemp, S.J. and Hards, V.L. 1999. *The mineralogy and microtextures of samples of the Mercia Mudstone Group from Northgates, Leicester*. British Geological Survey Technical Report, **WG/99/25C**.

Kemp, S.J., Ellis, M.A., Mounteney, I. and Kender, S. 2016*a*. Palaeoclimatic implications of high-resolution clay mineral assemblages preceding and across the onset of the Palaeocene–Eocene thermal maximum, North Sea Basin. *Clay Minerals*, **51**, 793–813, https://doi.org/10.1180/claymin.2016.051.5.08

Kemp, S.J., Smith, F.W. *et al.* 2016*b*. An improved approach to characterise potash-bearing evaporite deposits, evidenced in North Yorkshire, UK. *Economic Geology*, **111**, 719–742, https://doi.org/10.2113/econgeo.111.3.719

Labus, M. and Labus, K. 2018. Thermal conductivity and diffusivity of fine-grained sedimentary rocks. *Journal of Thermal Analysis and Calorimetry*, **132**, 1669–1676, https://doi.org/10.1007/s10973-018-7090-5

Merriman, R.J., Highley, D.E. and Cameron, D.G. 2003. *Definition and characteristics of very-fine grained sedimentary rocks: clay, mudstone, shale and slate*. British Geological Survey Commissioned Report, **CR/03/281N**.

Midttømme, K., Roaldset, E. and Aagaard, P. 1998. Thermal conductivity of selected claystones and mudstones from England. *Clay Minerals*, **33**, 131–145, https://doi.org/10.1180/000985598545327

Moore, D.M. and Reynolds, R.C. 1997. *X-Ray Diffraction and the Identification and Analysis of Clay Minerals*, 2nd edn. Oxford University Press, New York.

Ozbek, H. and Phillips, S. 1979. *Thermal conductivity of aqueous NaCl solutions from 20 °C to 330 °C*. University of California, Berkeley, LBL Report, **9086**.

Popov, Y., Pribnow, D.F.C., Sass, J.H., Williams, C. and Burkhardt, H. 1999. Characterization of rock thermal conductivity by high-resolution optical scanning. *Geothermics*, **28**, 253–276, https://doi.org/10.1016/S0375-6505(99)00007-3

Popov, Y., Bayuk, I., Parshin, A., Miklashevskiy, D., Novikov, S. and Chekhonin, E. 2012. New methods and instruments for determination of reservoir thermal properties. *Thirty-Seventh Workshop on Geothermal Reservoir Engineering, Stanford University, Stanford, CA, January 30–February 1, 2012*, **SGP-TR-194**.

Reynolds, R.C., Jr and Reynolds, R.C., III 2013. Description of Newmod II™. The calculation of one-dimensional X-ray diffraction patterns of mixed layered clay minerals. R. C. Reynolds, III, 1526 Farlow Avenue, Crofton, MD 21114.

Rollin, K.E. 1987. *Catalogue of geothermal data for the land area of the United Kingdom. Third revision: April 1987. Investigation of the Geothermal Potential of the UK*. British Geological Survey, Keyworth.

Snyder, R.L. and Bish, D.L. 1989. Quantitative analysis. *Reviews in Mineralogy. Mineralogical Society of America*, **20**, 101–144.

Vincent, C., Dashwood, B., Williams, J., Kuras, O., Kirk, K., Antcliff, P. and Barrett, M. 2019. *The UK GeoEnergy Test Bed, a Unique Geoscience Research Platform*. 81st EAGE Conference & Exhibition 2019, 3–6 June 2019, London, UK, 5.

Warrington, G., Audley-Charles, M.G. *et al.* 1980. *A correlation of Triassic rocks in the British Isles*. Geological Society of London, Special Report, **13**.

Wheildon, J., Gebski, J.S. and Thomas-Betts, A. 1985. *Further Investigations of the UK heat flow field (1981–1984). Investigation of the Geothermal Potential of the UK*. British Geological Survey, Keyworth.